Energy
Procedia

SHC 2015, International Conference on Solar Heating and Cooling for Buildings and Industry

Cost-optimal sizing of solar thermal and photovoltaic systems for the heating and cooling needs of a nearly Zero-Energy Building: the case study of a farm hostel in Italy

Daniele Testi, Eva Schito, Paolo Conti

BETTeR (Building Energy Technique and Technology Research group), University of Pisa – DESTEC, Largo Lucio Lazzarino, 56122 Pisa, Italy

Abstract

In this paper, the second of two parts, we apply the cost-optimal design method illustrated in Part 1 [1] to a case study. We select a farm hostel located in Enna, Italy, as the local climate and the required energy services are suitable for the development of a solar-assisted nearly zero-energy building. The system is connected to the electric grid and does not use any other thermal energy vector. Energy demand includes heating, cooling, domestic hot water production, lighting and other electric uses, viz. inductance cooking, food refrigeration, local dehumidification, household appliances, and office devices. The building-plant system is described in terms of both technical characteristics of each component and internal loads. According to the proposed simulation-based methodology, we investigate the best design configuration by minimizing the lifecycle cost after 20 years of operation. The results of the procedure identify the optimal solution, in terms of number of solar thermal and photovoltaic panels, volume and control strategy of the thermal storage. Other outputs are the dynamic and seasonal energy balance of each system component and of the whole system, and additional economic parameters. The results show that the proposed method leads to a very favorable design with relevant notable economic and energy benefits with respect to a no-solar design solution (ΔC^{TOT}=11%, ΔE_{IN}^{TOT}=67%). However, several nearly optimal configurations provide very similar outcomes in terms of lifecycle costs, with different initial investment and energy performances. Consequentially, we introduce a multi-objective optimization approach aimed at identifying the best solution in terms of investment availability and energy objectives.

Keywords: Nearly Zero-Energy Buildings; cost-optimal design; solar thermal; photovoltaics; heat pumps; case study

1. Introduction

In light of the energy uses for the building sector, current European Directives [2] focus on nearly Zero-Energy Buildings (NZEB), which are buildings characterized by very low energy need. Their high energy performance is

reached through a wise design of the envelope and efficient generation systems, together with the use of renewable sources for the production of both thermal and electrical energy.

Several research projects aim to find the optimal strategy to concurrently obtain high energy efficiency and low installation and operating costs [3,4]. In the first part of this work [1], we illustrated a methodology for the simulation of a solar-assisted NZEB system, consisting in a building envelope, a radiant floor, a heat pump (HP) unit, a thermal storage, solar thermal collectors (ST), and photovoltaic system (PV). A proper design of the whole system can be reached through the proposed "*simulation-based optimization procedure*", which provides as output the cost-optimal sizing of solar technologies and ancillary components (i.e. thermal storage), together with optimal control parameters. In the following sections, we describe the main features of the chosen case study and the results of the applied optimization procedure.

Nomenclature

Acronyms

BOS	balance of system
COP	coefficient of performance
CoSE	cost of saved energy
DHW	domestic hot water
FES	fractional energy savings (see definition in ISO 9488:1999 "Solar Energy – Vocabulary")
HP	heat pump
PER	primary energy ratio
PV	photovoltaic system
RF	radiant floor
ST	solar thermal system
TS	thermal storage

Symbols

C	global cost
C_0	installation cost
E	energy
F_R	ST removal factor
K_{RF}	RF thermal output per surface unit
$NOCT$	nominal operating cell temperature
$P_{th,des}$	peak load
S	surface
T_{off}	switching-off temperature
T_{TS}	thermal storage temperature
U	global heat transmittance of opaque walls
U_L	ST frontal losses coefficient
U_w	global heat transmittance of windows
U_{wf}	water-floor thermal transmittance
V	volume

b_0	incidence angle modifier coefficient for single-cover ST collectors
c_0	unitary installation cost
n	number of PV modules or ST collectors
s	thickness

Greek letters

$\beta_{T,PV}$	PV penalization factor depending on PV technology
η	efficiency
λ	thermal conductivity
$(\tau\alpha)_n$	transmittance-absorptance product for normal-incidence irradiance
ϕ	building time shift

Superscript

II	second-law parameter
$*$	sol-air temperature
TOT	cumulative value at the end of project lifetime

Subscript

el	electrical
$grid$	electrical grid
inv	electronic converter and other PV system components
ref	reference conditions
th	thermal
w	water

---

2. Description of the case study

The chosen design case study is a farm hostel in Enna, Sicily, Italy. As mentioned in [1], we developed models for each involved subsystem, viz. envelope thermal needs, radiant floor, air-to-water HP unit, PV generator, ST generator, and thermal energy storage. An hourly time step was chosen. In the following sections, we describe the main thermo-energetic features of each subsystem of the case study.

2.1. External climate

The city of Enna was chosen for its particular climate: at 931 m above sea level, winter is cold and summer is hot and sunny. These climate conditions, on one hand, cause the building high needs of thermal energy both for heating and cooling services but, on the other hand, are responsible for significant potential amount of energy provided by PV and ST generators. In addition, analyzing a farm hostel, there are also relevant demands of DHW.

Hourly profiles of external temperature, relative humidity and global solar irradiance on the horizontal plane are provided by CTI, Italian Thermotechnical Committee [5], and implemented for the simulation of the building energy demand. Table 1 shows the mean values of external temperature and global solar irradiance on the horizontal plane.

Table 1. External climate in Enna, Italy.

	Jan.	Feb.	Mar.	Apr.	May	Jun.	Jul.	Aug.	Sept.	Oct.	Nov.	Dec.
Mean external temperature [°C]	7.8	7.2	9.6	11.9	18.9	25.4	26.9	25.4	20.7	17.3	14.9	9.1
Global solar irradiance on the horizontal plane [kWh/m²]	0.27	0.25	0.35	0.35	0.45	0.44	0.46	0.47	0.39	0.32	0.22	0.23

2.2. Building envelope

The farm hostel is located in the mountain area, far enough away from the city. It is a two-story building, with a partially earth-sheltered zone (total height: *7.5 m* ; height of the earth-sheltered zone: *2 m* ; total floor area: *400 m²*). The envelope is realized with roughly squared ashlars, with a thickness of about 80 *cm*, (*U=0.82 W/(m²K)*), brick tiles insulated roofs (*U=0.3 W/(m²K)*; roof pitch: *12 deg*, facing west), insulated floor in concrete and tiles (*U=0.29 W/(m²K)*). These envelope elements are based on typical existing architecture in the mountain zone of Sicily [6], but we assumed that both roof and floor had been retrofitted. Double-glazed windows (*U_w=1.6 W/(m²K)*) have wooden frames and shutters (total windows area: *28.3 m²* , total glazed area: *20.2 m²*). Thermal bridges are taken into account with a 5% increase of the thermal transmittance of the opaque walls, as suggested by Italian Technical Standard UNI 11300-1:2008 [7]. Technical Standard UNI 10339:1995 [8] provides hourly air change rate for both infiltration and ventilation.

According to the methodology in [1], the hourly heating and cooling sensible loads are calculated using the following inputs:

- characteristic time shift of the building, $\bar{\phi} = 8$ h ;
- external temperature for a null heating demand, $T_{off,H} = 14$ °C ;
- external sol-air temperature for a null cooling demand, $T^*_{off,C} = 26$ °C ;
- design external temperature for heating, $T_{des} = -3$ °C ;
- design sol-air temperature for cooling, $T^*_{des,C} = 47$ °C ;
- peak load in both heating and cooling season, $P_{th,des} = 15$ kW

Internal air temperature is assumed to be constant and equal to 20°C and 26°C during heating and cooling mode, respectively.

2.3. Internal loads

The building can host up to 25 people, with 12 rooms, each of about 18 m². Users' presence is characterized by a summer peak: from June to September, the farm hostel is 60-80% full [9]. Moreover, a different schedule of presence during weekdays and weekend is assumed. The needs of domestic hot water and electrical energy due to typical household devices (e.g. personal computers, mini fridges, chargers) can be deduced on the basis of the hourly value of people's presence. These needs, together with the ones of electrical energy for cooking, are obviously higher during breakfast, lunch and dinner time [9]. People's presence also influences latent thermal loads and water vapor balance of the used spaces.

2.4. Radiant floor

As described in [1], we consider radiant floor as heat terminal unit. We evaluate RF heat transfer performance through the simplified resistance model described in Eqs. 6.a-6.b in [1]. The following parameters apply:

- mominal difference between the mean temperature of the water circulating within the radiant floor and internal air, $\Delta T_{RF,nom} = 20\ K$;
- radiant floor surface, $S_{RF} = 320\ m^2$;
- nominal thermal output per surface unit, $K_{RF,nom} = 60\ W/m^2$;
- emitter exponent, $n_{RF} = 1.1$;
- thermal conductance from the radiant floor to the water in the pipes, $U_{wf} = 6\ W/(m^2K)$.

2.5. Heat pump generator

In this case study, we consider an air-to-water HP unit with a nominal capacity of 16.5 kW in both heating and cooling mode. The hourly performance of the HP is calculated using the so-called *second-law efficiency*, as reported in [1]. According to typical values provided by manufacturers, $\eta_{HP,H}^{II}$ and $\eta_{HP,C}^{II}$ are 0.45 and 0.35, respectively. We adopt the same η_{HP}^{II} value for heating mode and DHW production. As described in [1], defrost cycles are performed when external temperature drops below 2°C. We consider an effective temperature difference between fluids at the HP outdoor/indoor heat exchangers equal to 10 and 5 K, respectively.

2.6. PV generator

In this case study, we consider standard monocrystalline-silicon panels. PV modules face South with a tilt angle of 12 deg . We evaluate PV performances through Eqs. 8.a-8.c described in [1]. The following parameters apply:

- efficiency of the electronic converter and other system components with losses (i.e. BOS), $\eta_{inv} = 0.85$;
- surface of each PV module, $S_{PV} = 1.5\ m^2$;
- temperature penalization factor for mono-Si PV, $\beta_{T,PV} = 0.004\ 1/K$;
- reference operational temperature of PV modules, $T_{ref,PV} = 25\ °C$;
- PV module efficiency at reference temperature, $\eta_{PV,ref} = 0.13$;
- nominal operation cell temperature, $NOCT = 45\ °C$.

2.7. ST Generator

In this case study, we consider flat-plate collectors. ST panels orientation and inclination are assumed to be equal to the ones of the PV panels. Thermal performances are evaluated through Eqs. 9.a-9.b described in [1]. The following parameters apply:

- surface of each ST collector, $S_{ST} = 3\ m^2$;
- ST removal factor, $F_R = 0.8$;
- transmittance-absorptance product for normal-incidence irradiance, $(\tau\alpha)_n = 0.7$;
- frontal losses coefficient, $U_L = 5\ W/(m^2K)$;
- incidence angle modifier coefficient for single-cover ST collectors, $b_0 = 0.1$.

2.8. Thermal storage

The energy balance of the thermal storage has been presented in Eqs. 10 and 11 in [1]. The temperature of the TS room is assumed to be equal to the annual average outdoor temperature (i.e. $T_{ext,TS} = 16.3\ °C$). The following parameters apply:

- nominal set-up temperature of the storage, $T_{TS,setpoint} = 50\ °C$;
- minimum TS temperature at which the heat pump is used to reheat the storage, $T_{TS,down} = 42\ °C$;
- maximum thermal storage water temperature, $T_{TS,max} = 90\ °C$;
- thermal conductivity of the thermal storage insulating material, $\lambda_{ST} = 0.04\ W/(mK)$;
- thickness of the thermal storage insulating material, $s_{ST} = 0.08\ m$.

According to the DHW load profile, we evaluate a minimum volume of 500 liters to ensure DHW service.

3. Simulation, optimization and design decisions

As above-mentioned, we evaluate both electrical and thermal energy balances for each hour of system operation over standard reference year (see Eqs. 12-13 in [1]). We aim at finding the optimal design in terms of minimum lifecycle cost (i.e. installation expenditure plus operational costs). The objective function is illustrated in Eq. 14 in [1] and shown again below.

$$C^{TOT} = c_{0,PV} n_{PV} + c_{0,ST} n_{ST} + c_{0,TS} V_{TS} + C_{0,HP} + \\ + \sum_{lifetime} \left\{ c_{el,in} \max\left[0; E_{el,grid}\right] + c_{el,out} \min\left[0; E_{el,grid}\right]\right\} \qquad [€] \qquad (1)$$

The optimization variables are n_{PV}, n_{ST}, V_{TS}, and $T_{TS,\mathrm{up}}$. Economic parameters are described in Table 2.

Table 2. Prices of electric energy and equipment.

Parameter	Value
Cost of the air-to-water HP, $C_{0,HP}$	12,000 €
Cost of each PV module, $c_{0,PV}$	700 €
Cost of each ST collector, $c_{0,ST}$	1 000 €
Cost of the thermal storage, $c_{0,TS}$	1 000 €/m³
Electrical energy grid buying price, $c_{el,in}$	0.20 €/kWh
Electrical energy grid selling price, $c_{el,out}$	0.10 €/kWh

Here, we apply an optimization procedure based on a simple *exhaustive enumeration method* [10] over the following vectors.

$$n_{ST} = \{0;1;2;4;6;8\} \qquad n_{PV} = \{0;5;10...55;60\}$$
$$V_{TS}\left[m^3\right] = \{0.5;1...4.5;5\} \qquad T_{TS,up}\left[°C\right] = \{50;55...65;70\}$$

Table 3 shows the optimal configuration and the corresponding value of C^{TOT}, together with some notable economic and energetic performance indexes (i.e. CoSE: ratio between installation costs and lifecycle saved energy with respect to the no-solar configuration; PER: ratio between the sum of useful energy outputs, in terms of primary energy, and the net primary energy input; FES: fractional energy savings with respect to the no-solar system, as defined by ISO 9488:1999). Besides, the same table shows the best configuration in terms of thermal and electrical energy delivered by solar technologies (the one with the lowest primary energy consumption).

Table 3. Objective functions and corresponding optimal design variables.

Objective function	Value	C_0 [k€]	CoSE [€/kWh]	PER	FES	$E_{in}{}^{TOT}$ [kWh/(m²y)]	n_{ST}	n_{PV}	$V_{TS}\left[m^3\right]$	$T_{TS,up}\left[°C\right]$
Lifecycle cost, C^{TOT}[k€]	72.1	41.0	0.39	3.8	0.67	34.9	4	35	0.5	70
Net primary energy consumption, $E_{in}{}^{TOT}$ [kWh/(m²y)]	-16.3	66.0	0.42	< 0 (positive energy building)	1.15	-16.3	8	60	4	50
No Solar Configuration	-	12.5	-	1.25	0	107.7	0	0	0.5	50

The optimal design, in terms of lifecycle cost, corresponds to 4 ST collectors, 35 PV panels, a TS of 500 liters (minimum allowed value) and a temperature for switching on/off the heat pump from direct heating mode of 70 °C (maximum allowed value). The small TS volume and the high value of $T_{TS,up}$ show that the best heating strategy is the direct coupling between HP generator and RF emitter. We can ascribe this outcome to the lower RF water temperature with respect to the TS one (see Fig. 1).
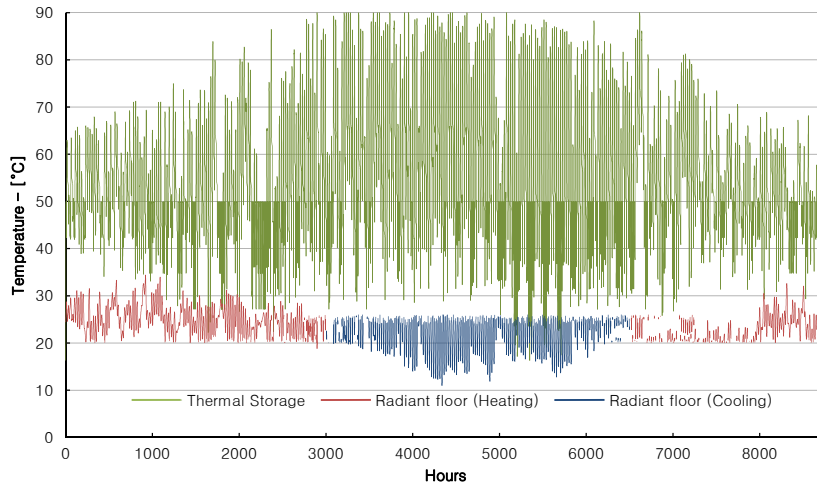

Fig. 1. TS and RF temperature evolution. With regard to RF, we do not show the time steps with null heating or cooling demand.

In this configuration, the ST generator delivers useful energy only for the DHW service (see Fig. 2.a). The optimal number of solar collectors corresponds to the best tradeoff between the cost reduction for TS recharge and ST installation costs. Similarly, the optimal number of PV modules depends on installation costs and the ratio between purchase and selling prices of electrical energy (see Table 2).

Fig. 2 shows the different shares of each generator on the various energy uses. Table 4 shows the ratio between the useful thermal energy output and the net electric energy input of the solar-assisted system for the three thermal services (system COP). Finally, Fig. 3 shows the overall thermal and electric energy demand shares.
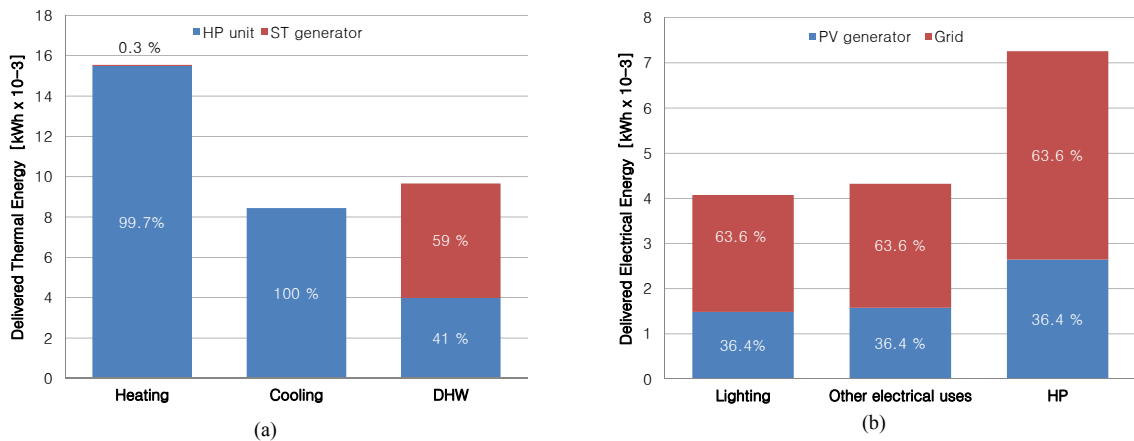

Fig. 2. Shares of thermal and electrical uses delivered by each generator.

Table 4. Overall COP (system COP) for each thermal service.

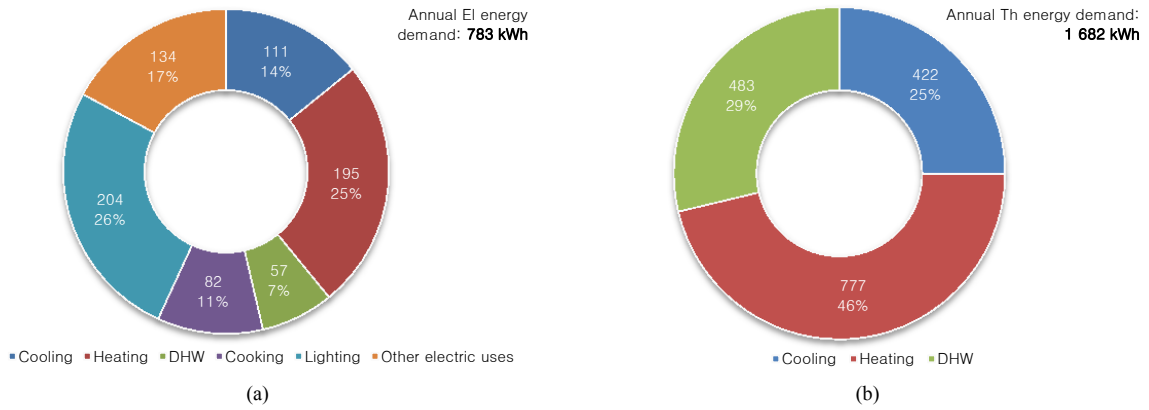|	Cooling	Heating	DHW
	3.8	4.0	8.5

Fig. 3. Electrical and thermal energy demand shares.

However, as already-introduced in [1], we aim at investigating the soundness of this optimal design, especially in terms of energy savings and installation costs. Fig. 4 shows the Pareto frontier of possible alternative solutions. The specifications of each point are reported in Table 5. In the latter table, we do not specify the TS volume and $T_{TS,up}$, because we verified a negligible influence of these two variables.
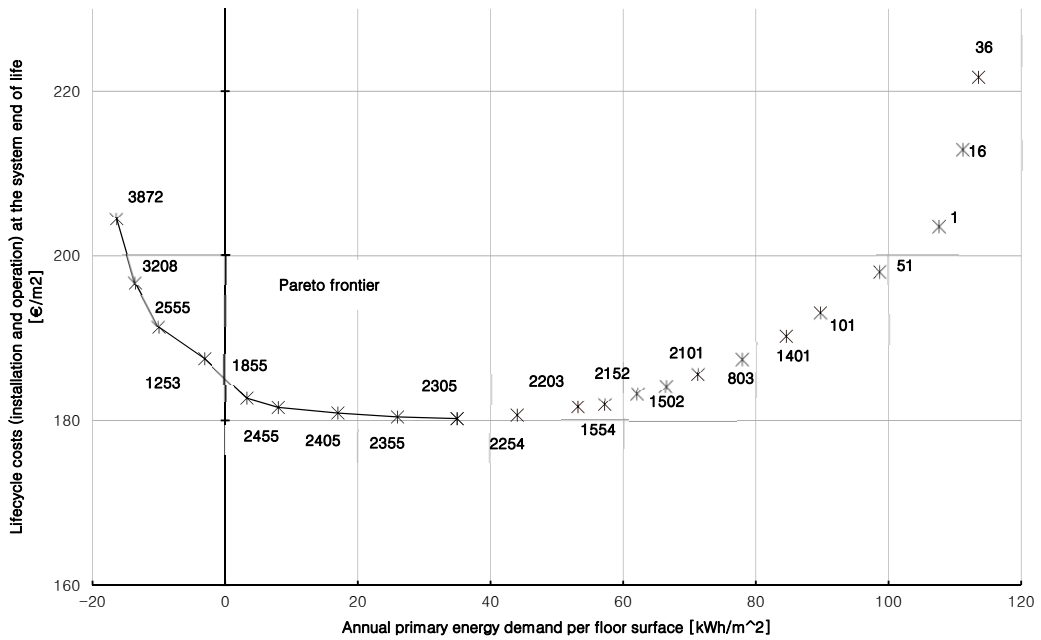

Fig. 4. Pareto frontier between C^{TOT} and E_{IN}^{TOT}.

Table 5. Design values and installation costs for the points on the Pareto frontier in Fig 5.

	Configuration number										
	3872	**3208**	**2555**	**1253**	**1855**	**2455**	**2405**	**2355**	**2305**	**2254**	**2203**
n_{ST}	8	6	4	1	2	4	4	4	4	4	4
n_{PV}	60	60	60	60	55	50	45	50	35	30	25
C_0 [k€]	64.5	61.0	58.5	55.5	53.0	51.5	48.0	44.0	41.0	37.5	34.0
	1554	**2152**	**1502**	**2101**	**803**	**1401**	**101**	**51**	**1**	**16**	**36**
n_{ST}	2	4	2	4	1	2	0	0	0	0	0
n_{PV}	25	20	20	15	15	10	10	5	0	0	0
C_0 [k€]	32.0	30.5	28.5	27.0	24.0	21.5	19.5	16.0	12.5	14.0	16.0

The curve in Fig. 4 presents a smooth profile in proximity of the actual cost-optimal point, with several nearly-optimum solutions. In other words, very different energy performances can be obtained at almost equal lifecycle costs. Consequently, a multi-criteria optimization seems necessary to guide the choice of the designer among possible alternative configurations. Obviously, it is not possible to define a unique criterion to select a universal best solution among the ones on the Pareto frontier. The choice on final design depends on the specific economic and regulatory framework. In other words, the final decision should consider also investment availability and possible limitations/objectives on energy performance of the building. In this context, Figs. 4-5 represent a useful tool in the decision-making process, showing installation costs as a function of primary energy demand.
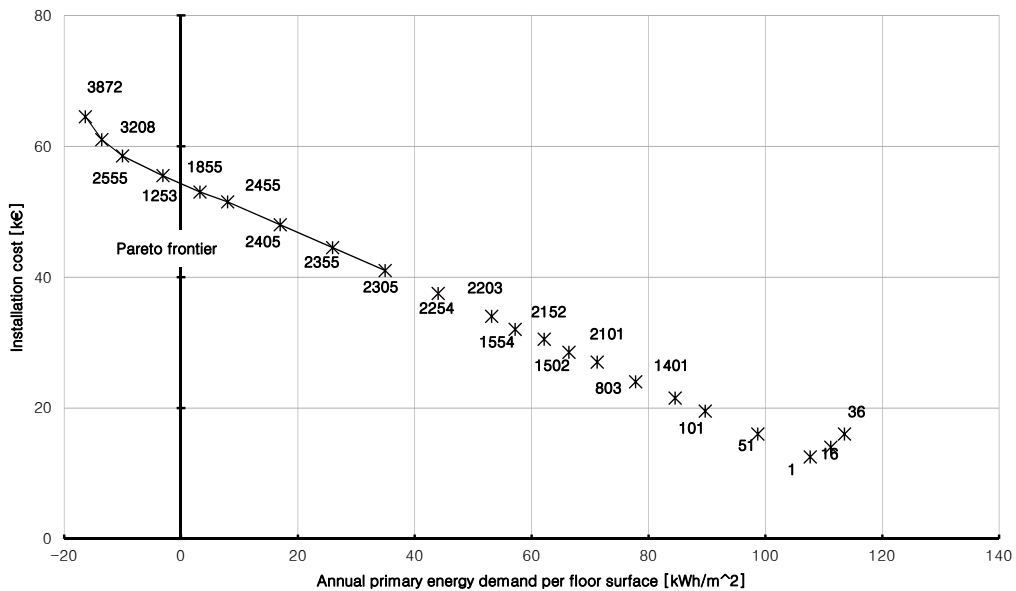

Fig. 5. Installation costs as a function of primary energy demand for the design solutions on the Pareto frontier in Fig. 4.

4. Conclusions

In the present work, we applied a simulation-based optimization methodology to a reference case: a solar-assisted nearly zero-energy farm hostel in Sicily. The results confirm that simulation-based optimization procedures represent an effective design tool for solar technologies and ancillary equipment (i.e. thermal storage), leading to favorable design and control strategies in terms of economic and primary energy savings. In this case study, we obtained a lifecycle cost reduction of 11% and a corresponding primary energy savings of 67%, with respect to a no-solar solution (i.e. air-to-water heat pump connected to the grid). The optimal design and control strategy match heating and cooling loads by means of the PV-assisted heat pump, while solar thermal collectors cover DHW demand.

With regard to a cost minimization goal, as described in Section 3, the optimal number of PV and ST modules strongly depend on a proper tradeoff among energy prices and installation costs. Moreover, we showed the existence of several nearly optimal configurations that lead to very similar economy savings, but very different investment costs and energy performances (see Figs. 4-5).

Consequently, we stress that the aim of this paper is not to provide a universal design criterion for solar-assisted buildings, but we encourage the use of the illustrated cost-optimal approach, together with multi-objective considerations. For this purpose, drawing charts similar to the ones in Figs. 4-5 can represent a useful tool, helping professionals to find the best design solution for the specific building and the actual economic and regulatory contexts. As a notable example, the method can be applied to meet the indications of current EU Directives on NZEBs and cost-optimal building design.

References

[1] Testi D, Schito E, Conti P. Cost-optimal sizing of solar thermal and photovoltaic systems for the heating and cooling needs of a nearly Zero-Energy Building: design methodology and model description. SHC 2015, Int. Conf. Sol. Heat. Cool. Build. Ind., Istanbul (TR): 2015.
[2] European Parliament and Council of the European Union. Directive 2010/31/EU on the Energy Performance of Buildings (Recast) 2010.
[3] Wright JA, Loosemore HA, Farmani R. Optimization of building thermal design and control by multi-criterion genetic algorithm. Energy Build 2002;34:959–72.
[4] Wang W, Zmeureanu R, Rivard H. Applying multi-objective genetic algorithms in green building design optimization. Build Environ 2005;40:1512–25.
[5] CTI. Typical Meteorological Year. Milan (IT): Italian Thermotechnical Committee (CTI); 2012.
[6] Bucci A, Mollo L. Regional Architecture in the Mediterranean Area. Florence (IT): Alinea Editrice; 2010.
[7] UNI/TS 11300-1, Energy performance of buildings - Part 1: Evaluation of energy need for space heating and cooling. Milan (IT): Italian National Unification; 2008.
[8] UNI 10339, Air-conditioning systems for thermal comfort in buildings - General, classification and requirements - Offer, order and supply specifications. Milan (IT): Italian National Unification; 1995.
[9] Aprile M. Caratterizzazione energetica del settore alberghiero in Italia (Energy uses in Italian hotels). Report RSE/2009/162 (in Italian); 2009.
[10] Venkataraman P. Applied Optimization with MATLAB Programming. Hoboken (NJ): John Wiley & Sons, Inc.; 2002.